ЖУРНАЛ СТРУКТУРНОЙ ХИМИИ

2017. Том 58, № 2 *Февраль – март* *С. 278 – 284*

UDC 541.6:543.422:548:737

THEORETICAL INVESTIGATION OF THE MOLECULAR STRUCTURE AND SPECTROSCOPIC PROPERTIES OF OXICAMS

A.G. Pacheco[1], G. Salgado-Morán[2], L. Gerli-Candia[3], R. Ramírez-Tagle[4], D. Glossman-Mitnik[5], A. Misra[6], A.F. de Carvalho Alcântara[7]

[1]*Instituto Federal de Educação Ciência e Tecnologia do Sul de Minas Gerais, Inconfidentes, Brasil*
[2]*Departamento de Ciencias, Facultad de Ciencias Exactas, Universidad Andrés Bello, Concepción, Chile*
[3]*Departamento de Química Ambiental, Facultad de Ciencias, Universidad Católica de la Santísima Concepción, Concepción, Chile*
[4]*Facultad de Ingeniería, Ciencia y Tecnología, Universidad Bernardo O'Higgins, Santiago, Chile*
E-mail: rramirez@ubo.cl
[5]*Laboratorio Virtual NANOCOSMOS, Centro de Investigación em Materiales Avanzados, Chihuahua, Mexico*
[6]*Vidyasagar University, Midnapore, India*
[7]*Universidade Federal de Minas Gerais, Belo Horizonte, Brasil*

Received June, 23, 2015 *Revised — December, 30, 2015*

Nonsteroidal anti-inflammatory drugs (NSAIDs) are among the most frequently prescribed drugs and have multiple therapeutic uses. These drugs are predominantly used for the treatment of musculoskeletal diseases because of their analgesic, antipyretic, and antiplatelet activities. Oxicams constitute an interesting class of organic compounds and have been investigated in the search for new analgesic and anti-inflammatory drugs. In the present work, a theoretical investigation of the molecular structure and spectroscopic properties of a series of five oxicams in different solvents was performed using density functional theory (DFT) methods. The geometric optimizations of the oxicams were carried out using the M06 density functional and the CBSB7 basis set. The infrared data were all obtained at the same theoretical level. The UV-Vis absorption and NMR data of some oxicams were calculated using the DFT and CBSB3 basis sets. The analysis of structural parameters, particularly the bond length and spectroscopic data, indicated that interactions occurred between the hydrogen bond types for 4-meloxicam, isoxicam, and normeloxicam. Stereoelectronic interactions caused by the substitution of alkyl groups caused the bond lengths to elongate. Similarly, the substitution of heteroatoms, such as nitrogen, sulfur, or oxygen, increased the bond lengths and angular stresses.

DOI: 10.15372/JSC20170206

K e y w o r d s: nonsteroidal anti-inflammatory drugs, chemical properties, spectroscopic analysis, density functional theory.

INTRODUCTION

Nonsteroidal anti-inflammatory drugs (NSAIDs) have various therapeutic uses, including for the treatment of musculoskeletal diseases, because of their analgesic, antipyretic, anti-inflammatory, and antiplatelet activities [1]. However, their use is limited by their potential adverse effects, such as pepticulcers or renal failure. Both adverse effects and potential toxicity are due to the inhibition of the cyclooxygenase (COX) enzyme, which causes the inhibition of thromboxanes and prostaglandins

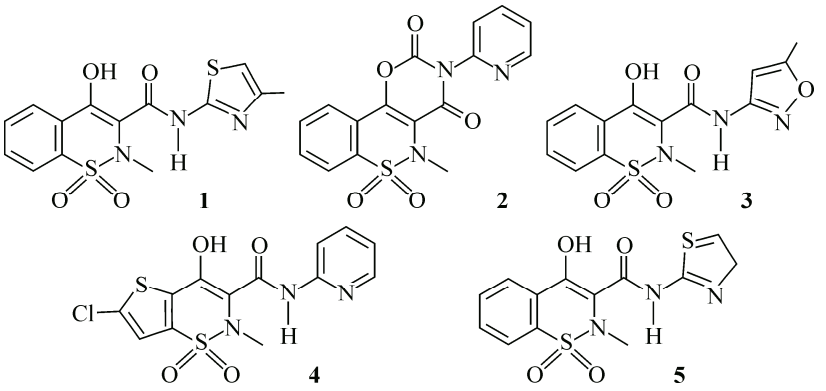

Fig. 1. Structure of oxicams studied by DFT and TD-DFT using the M06 density functional as well as the CBSB7 and CBSB3 basis sets (**1** = 4-meloxicam, **2** = droxicam, **3** = isoxicam, **4** = lornoxicam, **5** = normeloxicam)

(PGs). PGH_2 synthase exhibits two catalytic activity paths: cyclooxygenase and peroxidase. NSAIDs inhibit the activity of COX, but do not inhibit the activity of the peroxidase enzyme.

Oxicams are enolcarboxamides that contain the 4-hydroxy-1,2-benzothiazines-3-carboxamide 1,1-dioxide group in their skeletons. These compounds exhibit interesting pharmacological properties since they are a class of NSAIDs characterized by a long duration of action [2]. Piroxicam and meloxicam derived from oxicam are eight times more selective for COX-2 than oxicam and have few clinical side effects at the gastrointestinal level [3].

Rofecoxib is an NSAID of the oxicam class. This product was removed from the market because it increased the risk of heart attack and stroke. Subsequently, other derivatives of this chemical class family, such as parecoxib, valdecoxib, and lumiracoxib, were recalled due to their pharmacologic side effects [4].This fact justifies the search for new analgesics and anti-inflammatory drugs based on oxicam derivatives with better therapeutic properties.

They are effective in the treatment of rheumatoid arthritis, osteoarthritis, postoperative pain, and degenerative joint diseases. Furthermore, these compounds also display chemopreventive and chemosuppresive effects against various cancer cell lines and therefore represent an important class of versatile pharmaceutical drugs. The DFT approach has been applied to predict the pK_a of several synthesized oxicam derivatives [5].

The studies performed in the liposomes/water systems proved that, in spite of structural similarities, oxicams present different interactions with lipid membranes and the found correlations between interactions with membranes; ionization forms and COX inhibition are relevant to understand the pharmacological effects of these oxicams [6].

In a previous work, we have shown that the spectroscopic properties of oxicams are heavily influenced by the solvent used in the analysis [7, 8]. The underlying solvent has a considerable effect on the oxidation potentials of the oxicams and, hence, on their antioxidant activity, mainly by affecting the solvation of their more polar intermediates in the electrochemical calculations [9].

In the present work, the molecular structure and spectroscopic properties of five oxicams (Fig. 1) have been studied in different solvents using DFT and TD-DFT methods and the M06 suite of functionals in conjunction with the CBSB7 and CBSB3 basis sets. The results were analyzed and correlated to the available experimental results.

METHODS AND COMPUTATIONAL DETAILS

Theoretical calculations were performed using the DFT methods implemented in the Gaussian 09 computational package [10]. The equilibrium geometries were determined by the generalized gradient technique. The force constants and vibrational frequencies were determined by computing the analytical frequencies at the stationary points obtained from the geometry optimization. The optimized geometries were characterized as true minima on the potential energy surface (PES) when all of the har-

monic frequencies were real. The molecular structure and properties were calculated using the M06 functional suite, which is a set of four meta-*hybrid G*GA density functionals that provides consistent and satisfactory results for several structural and thermodynamic properties [11—13].

Geometric optimization and calculation of the vibrational mode frequencies and intensities of the infrared spectra were performed based on the CBSB7 basis sets (equivalent to 6-311G (2*d*,*d*,*p*)). Other electronic properties were calculated with the CBSB3 basis sets (equivalent to 6-311++G(2*d*,*f*,2*p*)). The CBS methods adequately seek the solutions of the Schrödinger equation for small and medium sized molecules. These methods calculate the total energy with a high degree of accuracy (~1.2 kcal/mol), meaning that they are suitable for *ab initio* calculations of electronic structures [14—16].

Solvation energies were computed by the integral equation formalism-polarizable continuum model (IEF-PCM) [17], including the UAKS model for water, methanol, ethanol, 1,4-dioxane, dimethylsulfoxide, and N,N-dimethylformamide.

The calculation of UV-Vis data was performed by solving the time-dependent DFT (TD-DFT) equations according to the method implemented in Gaussian 09 [18—21]. The infrared (IR) and ultraviolet (UV-Vis) data were calculated with the Swizard [22, 23] program and visualized with Gabedit [24]. In all cases, the spectra show the calculated frequencies and absorption or emission wavelengths. The NMR spectra and magnetic properties were calculated using the M06 density functional with the CBSB3 basis set. The NMR spectra and magnetic properties were visualized and analyzed using GaussView 5.0.

RESULTS AND DISCUSSION

The spectroscopic techniques are widely accepted as non-invasive techniques to investigate the behavior of drugs in different solvents, including their interactions with macromolecules. Such studies can yield a wide array of information relating to the structure, dynamics, energy, and related properties of individual molecules as well as the interactions that occur when molecules are solvated by a solvent. Oxicams are extremely sensitive to their microenvironments, which makes their spectral parameters strongly dependent on the corresponding solvents [25].

Structural parameters. The optimized geometries of **1**—**5** (Fig. 2), obtained with the M06 density functional and the CBSB7 basis set, present similar structural parameters because their structures differ only in the aromatic ring. By analyzing each compound, it can be observed that the substitution of hydrogen atoms with alkyl groups in the oxicam structures increases the length of the replaced bond. In a similar fashion, the presence of heteroatoms also increases the length of the replaced bond. This can be attributed to the interaction between the electronic structure and stereochemistry of a molecule (stereo electronic effects), which occurs in the electron clouds of the substituent group and the bond atom. As such, the chemical bond length increases to reduce the stereo electronic effects. Additionally, a lengthening of the bond when the carbon atom is replaced by the heteroatom (sulfur specifically) is observed because of nuclear repulsion; since the heteroatom has a larger atomic radius than carbon, the bond length increases. Some of the structures exhibit typical hydrogen bond interactions.

For the specific case of the structure of 4-meloxicam (**1**), the bonds corresponding to R(8—22) and R(17—23), which are formed between carbon atoms and sulfur, increase in length due to the higher atomic radius of sulfur, which in turn increases the repulsion. Additionally, the increase in the bond length at R(6—21) clearly shows the stereotype electronic interaction of the methyl group. In this way, the angles corresponding to C8—S22—C9 (1.537 rad or 88.1°) and C17—S23—N21 (1.742 rad or 99.8°) cause angular tension between these atoms. The C14 atom of (**1**) presents a sp^2 hybridization and is attached to the oxygen atom (O13) in a planar structure. The O12 atom is 0.0992 nm from the H32 atom, indicating a typical hydrogen bond. This bond is supported by 0.1693 nm bond between O13 and H32. The 1.759 rad angle between C14, H32, and O13 results in a considerable angular strain.

The droxicam (**2**) molecule exhibits the effects of increasing bond lengths corresponding to R(9—20), which presents an electronic stereo effect due to the alkyl substituent. This can also be seen in R(10—23) between carbon and nitrogen atoms; in R(12—25) and R(13—25) between oxygen and sulfur atoms due to interactions between heteroatoms, such as R(20—25) between nitrogen and sulfur

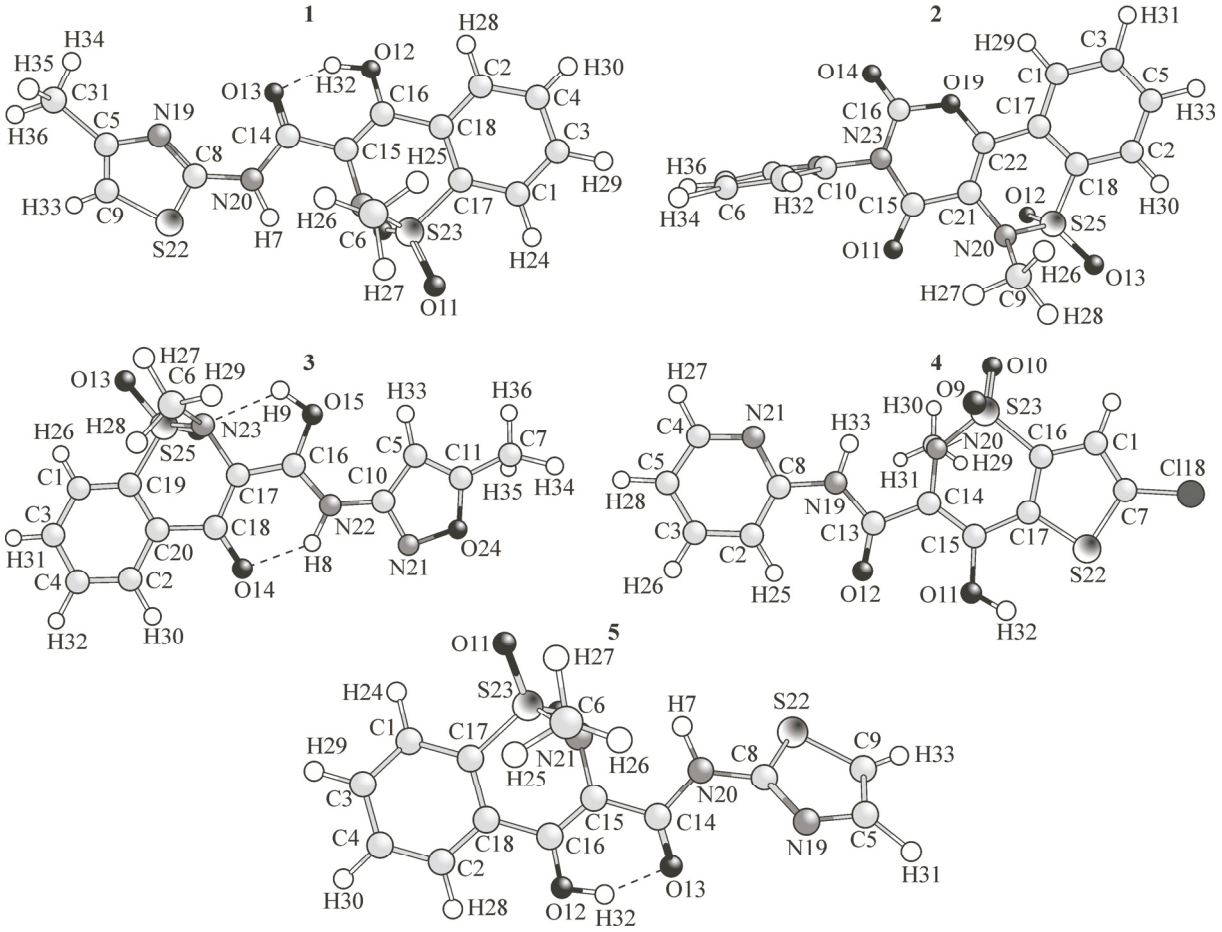

Fig. 2. Optimized structures of oxicams **1**—**5** calculated with the M06 density functional and the CBSB7 basis set (showing the numbering used in this work and determined by the calculation software)

atoms; and in R(18—25) between carbon and sulfur atoms. This is evidenced by a bond angle of 1.752 rad (100.4°), resulting in a strong angular tension between C18—S25—N20.

The isoxicam (**3**) molecule shows hydrogen bond type interactions with bond lengths of 0.1866 and 0.2046 nm between O14—H8 and N23—H9, respectively.

This interaction results in an angular strain between C17—N23—H9 and C18—O14—H8, which is caused by angles of 1.398 rad (80.1°) and 1.787 rad (102.4°), respectively. Additionally, it is possible to observe elongated bond lengths, as in the above structures, including N23—C6, C19—S25, and N23—S25 bonds, due to stereo-electronic and nuclear repulsion effects.

The structure of lornoxicam (**4**) includes a chlorine heteroatom which is highly electronegative. This gives unique characteristics, such as a high electron density, that translate into an elongation of the bond formed between C7—Cl18 (0.1712 nm). Similar to the previously mentioned structures, the C6—N20 bond elongates due to the stereo-electronic and nuclear repulsion (0.1468 nm).

In addition, C7 binds to the second heteroatom, sulfur, which elongates the C7—S22 bond (0.1732 nm), leading to bond angles of 1.581 rad (90.6°) and 1.723 rad (98.7°), respectively, and angular tensions between C7—S22—C17 and C16—S23—N20.

In normeloxicam (**5**), the H32 and O13 atoms have a bond length of 0.1698 nm and show hydrogen bonding interactions, resulting in a O13—H32—C14 bond angle of 1.758 rad (100.7°). Similarly to the other molecules investigated in this study, this structure presents elongated bond lengths due to alkyl group substitutions or bonds between carbon and heteroatoms, particularly sulfur. The bonds between C8—S22—C9 and C17—S23—N21 result in highly stressed angles of 1.541 rad (88.3°) and 1.740 rad (99.7°), respectively.

IR and UV-Vis absorption spectra. The infrared spectra calculated with the M06 density function and the CBSB7 basis set as well as the absorption spectra of the five oxicams in six different solvents calculated with TD-DFT and the M06 density function coupled to the CBSB3 basis set indicate that the intensity of an absorption band depends on the polarity of the bond.

The absorption intensity increased with increasing polarization of the chemical bonds. This is also true for the absorption spectra obtained using various solvents, namely, water, methanol, ethanol, 1,4-dioxane, dimethylsulfoxide, and N,N-dimethylformamide. Aromatic rings, amide, carbonyl, hydroxyl, and amino groups in the structure of the studied compounds lead to transitions of several types, such as $\pi \rightarrow \pi^*$ and $n \rightarrow \pi^*$, between180 nm and 370 nm. An increase in the solvent polarity, indicated by a larger dielectric constant (ε), shifted the $n \rightarrow \pi^*$ transitions to lower wavelengths (increased energy and hypsochromic shift) and caused bathochromic shifts to $\pi \rightarrow \pi^*$ transitions. The location and intensity of the bands depend on the substituents present in the structure, which shift the absorption peak of the chromophore to longer wavelengths (hypsochromic effect) or to lower wavelengths (bathochromic effect) and possibly varies the intensity. All of the calculated electronic transitions and hypsochromic/bathochromic shift effects are in good agreement with the observed experimental values [26].

The IR spectrum of 4-meloxicam (**1**) has bands between 3300 and 3400 cm^{-1}, which are attributed to absorptions of hydroxyl and secondary amide groups. The absorption near 1572 cm^{-1} is characteristic of the second arylamide. The absorption at 1180 cm^{-1} is characteristic of an S=O group. The absorption at 600 cm^{-1} is characteristic of sulfur heteroatom bonds. From the UV-Vis absorption spectra, it can be observed that the increasing polarity of the solvent caused a hypsochromic effect that favored the formation of hydrogen bonds in the molecule.

Droxicam (**2**): the IR spectrum presents two sharp peaks between 1780 and 1900 cm^{-1} which correspond to carbonyl groups (C15—O11 and C16—O14). These two signals were displaced due to the difference in the chemical environments that were tested. The absorption related to the C15—O11 bond shifted to a higher frequency due to the delocalization of π electrons between its neighboring atoms. At approximately 1450 cm^{-1}, the spectrum shows a sharp peak that is characteristic of the SO_2 group. By analyzing the UV-Vis absorption spectra (Fig. 2, **2**), transitions of $\pi^* \rightarrow n$ type from 200 to 315 nm and also characteristic absorption at approximately 280 nm, which corresponds to the carbonyl groups, can be observed.

Isoxicam (**3**): Absorption bands characteristic of hydrogen bonds (3650 and 3300 cm^{-1}) can be observed in the IR spectrum. These interactions were observed in the absorption spectra for the solvents with higher dielectric constants. Fig. 2, **3** shows that the absorption bands are narrower and more pronounced in the more polar solvents.

Lornoxicam (**4**): The characteristic absorptions of amide (1793 cm^{-1}) and bound C—Cl (800—600 cm^{-1}) can be observed. The two bonds with the sulfur heteroatom C17—C16—S22 and C17—C16—S23 have different chemical environments. The C17—C16—S22 group is influenced by the electronegative chlorine atom and the absorption band moves toward 1470 cm^{-1}, whereas the S23 atom is bonded to two oxygen atoms and one nitrogen atom, which causes a strong signal of approximately 1570 cm^{-1} and other absorption bands characteristic of sulfonamide (1180 cm^{-1}). An absorption band corresponding to the hydroxyl group attached to C15 located at approximately 1150 cm^{-1} can also be observed.

An analysis of the absorption spectra (Fig. 2, **4**) clearly shows the effect of the solvent polarity in the positions of the peaks. For example, for solvents with a higher dielectric constant than that of 1,4-dioxane, the spectra display two notable signals, whereas the spectrum in the presence of 1,4-dioxane, which has a dielectric constant (ε) of 2.25, shows a broadening and deformation of the absorption bands due to hypsochromic and bathochromic shifts in the system.

Normeloxicam (**5**): the IR spectra of **5** show peaks characteristic of hydrogen bond interactions and absorptions of sulfonamide, amide, and enol groups. These are favorably observed in the UV-Vis absorption spectra with higher dielectric constants (Fig. 2, **5**) and narrow spectra corresponding to the $n \rightarrow \pi^*$ and $\pi \rightarrow \pi^*$ transitions (hypsochromic and bathochromic shifts, respectively). Furthermore,

because of the electron delocalization in the atomic centers of the anti-bonding molecular orbital, the energy decreases so that the absorption maxima shift to longer wavelengths.

CONCLUSIONS

The analysis of structural parameters indicates hydrogen bond interactions between the adjacent hydrogen and oxygen atoms, which is evidenced by an appropriate length for this type of interactions. The structures of 4-meloxicam, isoxicam, and normeloxicam yield interactions similar to those with hydrogen bonds. The replacement of a hydrogen atom by an alkyl group in the studied structures elongated the corresponding bond length. This effect can be attributed to stereoelectronic interactions because of the substituent size. Heteroatom (nitrogen, sulfur or oxygen) substitution for carbon atoms in the molecular structure increases the bond lengths and angular stresses.

The absorption spectra of these molecules exhibit a peak of approximately 1571 cm^{-1}, corresponding to the carbonyl group, which is displaced to lower frequencies due to the electron delocalization. The absorption band intensities also increase with the polarity of the bonds. The transitions observed in the molecules correspond to $\pi \rightarrow \pi^*$ and $n \rightarrow \pi^*$ electronic transitions. The increasing solvent polarity caused hypsochromic displacements at the bands corresponding to $n \rightarrow \pi^*$ transitions, while the $\pi \rightarrow \pi^*$ transitions moved to longer wavelengths (bathochromic shift).

As a result of the electron delocalization, the anti-bonding MO energy decreased so that the absorption maxima shifted to longer wavelengths. The calculated electronic transitions as well as the hypsochromic and bathochromic shift effects are in good agreement with the observed, averaged experimental values.

The variations observed in the IR and UV-Vis spectra may be related to the different structures involved in the tautomeric equilibrium in the tested media. A particular structure involved in keto-enol tautomerism can be favored depending on the polarity of the medium, which also determines the anti-inflammatory activity of the structures studied [5, 6, 9].

The bond length and bond angle data of the optimized molecular structures, as well as the IR and UV-Vis spectra of the systems used in this work, are available in the supplementary material.

This work has been supported by CIMAV, SC, Consejo Nacional de Cienciay Tecnología (CONACYT, Mexico) and Federal Institute of Education Science and Technology of South of Minas Gerais — Inconfidentes (IFSULDEMINAS). R. Ramírez-Tagle gratefully acknowledges the financial support from Fondecyt 1130007 The authors are grateful to R. Arratia for his valuable assistance.

REFERENCES

1. *Cronstein B., Weissmann G.* // Ann. Rev. Pharmacol. Toxicol. – 1995. – **35**. – P. 449.
2. *Lazer E., Miao C., Cywin C., Sorcek R., Wong H., Meng Z., Potocki I., Hoermann M., Snow R., Tschantz M., Kelly T., McNeil D., Coutts S., Churchill L., Graham A., David E., Grob P., Engel W., Meier H., Trummlitz G.* // J. Med. Chem. – 1997. – **40**. – P. 980.
3. *Bianchi M., Panerai A.* // Pharmacol. Res. – 2002. – **45**. – P. 101.
4. *Dogn'e J., Supur'an C., Pratico D.* // J. Med. Chem. – 2005. – **48**. – P. 2251.
5. *Ho J., Coote M.L., Franco-Perez M., Gomez-Balderas R.* // J. Phys. Chem. A. – 2010. – **11992**. – P. 114.
6. *Lúcio M., Ferreira H., Lima J.L.F.C., Reis S.* // Med. Chem. – 2006. – **447**. – P. 2.
7. *Martínez-Araya J., Salgado-Moran G., Glossman-Mitnik D.* // J. Phys. Chem. B. – 2013. – **6339**. – P. 117.
8. *Salgado-Moran G., Gerli-Candia L., Martinez-Araya J., Ramirez-Tagle R., Glossman-Mitnik D.* // Int. J. Pharm. Bio. Sci. – 2013. – **374**. – P. 4.
9. *Ghaempanah A., Jameh-Bozorghi S., Darvishpour M., Fekri M.H.* // Int. J. Electrochem. Sci. – 2012. – **6127**. – P. 7.
10. *Frisch M.J., Trucks G.W., Schlegel H.B., Scuseria G.E., Robb M.A., Cheeseman J.R., Scalmani G., Barone V., Mennucci B., Petersson G.A., Nakatsuji H., Caricato M., Li X., Hratchian H.P., Izmaylov H.F., Bloino J., Zheng G., Sonnenberg J.L., Hada M., Ehara M., Toyota K., Fukuda R., Hasegawa J., Ishida M., Nakajima T., Honda Y., Kitao O., Nakai H., Vreven T., Montgomery J.A., Peralta J.E., Ogliaro F., Bearpark M., Heyd J.J., Brothers E., Kudin K.N., Staroverov V.N., Kobayashi R., Normand J., Raghavachari K., Rendell A., Burant J.C., Iyengar S.S., Tomasi J., Cossi M., Rega N., Millam J.M., Klene M., Knox J.E., Cross J.B., Bakken V.,*

Adamo C., Jaramillo J., Gomperts R., Stratmann R.E., Yazyev O., Austin A.J., Cammi R., Pomelli C., Ochterski J.W., Martin R.L., Morokuma K., Zakrzewski V.G., Voth G.A., Salvador P., Dannenberg J.J., Dapprich S., Daniels A.D., Farkas A., Foresman J.B., Ortiz J.V., Cioslowski J., Fox D.J. Gaussian 09, Revision A.1. Program for quantum chemical calculations. – Wallingford, CT: Gaussian Inc., 2009.

11. *Zhao Y., Truhlar D.G.* // Acc. Chem. Res. – 2008. – **41**. – P. 157.
12. *Zhao Y., Truhlar D.G.* // Theor. Chem. Acc. – 2008. – **120**. – P. 215.
13. *Zhao Y., Truhlar D.G.* // Chem. Phys. Lett. – 2011. – **502**. – P. 1.
14. *Montgomery J., Frisch M., Ochterski J., Petersson G.* // J. Chem. Phys. – 1999. – **110**. – P. 2822.
15. *Montgomery J., Frisch M., Ochterski J., Petersson G.* // J. Chem. Phys. – 2000. – **112**. – P. 6532.
16. *Tomasi J., Mennucci B., Cances E.* // J. Mol. Struct.: THEOCHEM. – 1999. – **464**. – P. 211.
17. *Emel'yanenko V.N., Verevkin S.P., Burakova E.N., Roganov G.N., Georgieva M.K.* // Russ. J. Phys. Chem. A. – 2009. – **83**. – P. 697.
18. *Lewars E.* Computational Chemistry — Introduction to the Theory and Applications of Molecular and Quantum Mechanics. – Dordrecht: Kluwer Academic Publishers, 2003.
19. *Stratmann R., Scuseria G., Frisch M.* // J. Chem. Phys. – 1998. – **109**. – P. 8218.
20. *Bauernschmitt R., Ahlrichs R.* // Chem. Phys. Lett. – 1996. – **256**. – P. 454.
21. *Casida M.E., Jamorski C., Casida K.C., Salahub D.R.* // J. Chem. Phys. – 1998. – **108**. – P. 4439.
22. *Swizard* Program Revision 4.6. Program for Postprocessing of Spectral Data. – Canada: University of Ottawa, 2010.
23. *Gorelsky S., Lever A.* // J. Organomet. Chem. – 2001. – **635**. – P. 187.
24. *Allouche A.* // J. Comp. Chem. – 2011. – **32**. – P. 174.
25. *Ghaenpanah A., Jameh-Bozorghi S., Darvisshpour M., Fekri M.* // Int. J. Electrochem. Sci. – 2012. – **7**. – P. 6127.
26. *Banerjee R., Chakraborty H., Sarkar M.* // Spectrochim. Acta, Part A. – 2003. – **59**. – P. 1213.